



CHORUS

This is the accepted manuscript made available via CHORUS. The article has been published as:

Parity-time-symmetric teleportation

Y. Ra'di, D. L. Sounas, A. Alù, and S. A. Tretyakov

Phys. Rev. B **93**, 235427 — Published 15 June 2016

DOI: [10.1103/PhysRevB.93.235427](https://doi.org/10.1103/PhysRevB.93.235427)

Parity-Time-Symmetric Teleportation

Y. Ra'adi^{1,2}, D. L. Sounas³, A. Alù³, and S. A. Tretyakov²

¹*Department of Electrical Engineering and Computer Science,
University of Michigan, Ann Arbor, Michigan 48109, USA*

²*Department of Radio Science and Engineering, Aalto University, P.O. Box 13000, FI-00076 Aalto, Finland*

³*Department of Electrical & Computer Engineering,
The University of Texas at Austin, Austin, Texas 78701, USA*

We show that electromagnetic plane waves can be fully “teleported” through thin, nearly fully reflective sheets, assisted by a pair of parity-time-symmetric lossy and active sheets in front and behind the screen. The proposed structure is able to almost perfectly absorb incident waves over a wide range of frequency and incidence angles, while waves having a specific frequency and incidence angle are replicated behind the structure in sync with the input signal. It is shown that the proposed structure can be designed to teleport waves at any desired frequency and incidence angle. Furthermore, we generalize the proposed concept to the case of teleportation of electromagnetic waves over electrically long distances, enabling full absorption at one surface and the synthesis of the same signal at another point located electrically far away from the first surface. The physical principle behind this selective teleportation is discussed, and similarities and differences with tunneling and cloaking concepts based on \mathcal{PT} -symmetry are investigated. From the application point of view, the proposed structure works as an extremely selective filter, both in frequency and spatial domains.

I. INTRODUCTION

The phenomenon of tunneling of electromagnetic waves through opaque layers has always been a fascinating and somehow counterintuitive subject. Tunneling structures based on an extremely high negative permittivity layer coated by high positive permittivity layers [1], a negative permittivity slab sandwiched between birefringence layers [2], conjugate matched pair of negative permittivity and negative permeability slabs [3], a negative permittivity slab paired with a double-positive uniaxial slab [4], and permittivity-near-zero bi-layers [5] have been reported. Recently, it was revealed that the phenomenon of electromagnetic wave tunneling can happen through electrically long distances [6]. However, in all these scenarios it is the incident energy itself that tunnels through the structure and reaches the other side. Would it be possible instead to “teleport” the incident electromagnetic wave from the input of the structure to its output without opening any tunnel through opaque objects? In other words, can we design a structure that absorbs electromagnetic waves at one surface and recreates it with the same properties at another place far away from the first surface?

In the last few years significant research efforts have been devoted to explore the properties of a new class of artificial materials and structures based on parity-time (\mathcal{PT})-symmetric systems, e.g. [7, 8]. These structures allow control over the dissipation and power amplification inside the system, while, under appropriate conditions, the overall response remains lossless. Scattering characteristics of several \mathcal{PT} -symmetrical structures have been explored [9–12]. Recently, a unidirectional cloaking structure based on \mathcal{PT} -symmetric metasurfaces was introduced [13]. In that system, the illuminated half of the structure, which is lossy, fully absorbs the impinging power, and the other half, which is active, self-tunes

itself over time to reproduce the incident wave behind the structure. In this configuration, the small coupling between the lossy and active regions due to edge diffraction is found to be enough to synchronize the active part and ensure that the incident wave is recreated. Inspired by this work, here we propose and investigate the idea of \mathcal{PT} -symmetric teleportation through extremely opaque layers.

II. CONTROL OVER REFLECTION AND TRANSMISSION

Let us consider a thin, nearly ideally conducting film with a very small surface reactance (e.g., an ideally conducting layer perforated with a two-dimensional sub-wavelength array of tiny holes). First, we consider a particular example of a normally incident electromagnetic plane wave with the wavelength $\lambda_0 = 30$ mm on the film with a very low surface impedance $Z_s = j0.01$ Ohm. This inductive sheet behaves nearly as a perfect mirror: it reflects 99.99997 % of the incident power and allows transmission of only a negligible amount of the impinging power, in this example, 0.00003 %. Therefore, the screen creates a very strong reflection and a deep shadow behind it. Going step by step, we will discuss how one can eliminate reflections, shadow, and make the total scattered power identically zero (realizing the teleportation regime) for such a strong reflector, based on \mathcal{PT} -symmetry.

A. Engineering Reflection

Reflections from a mirror can be eliminated using an absorber. To this end, one can simply position a resistive sheet in front of the inductive layer, as in a Salisbury absorber [14]. Since the screen has a negligi-

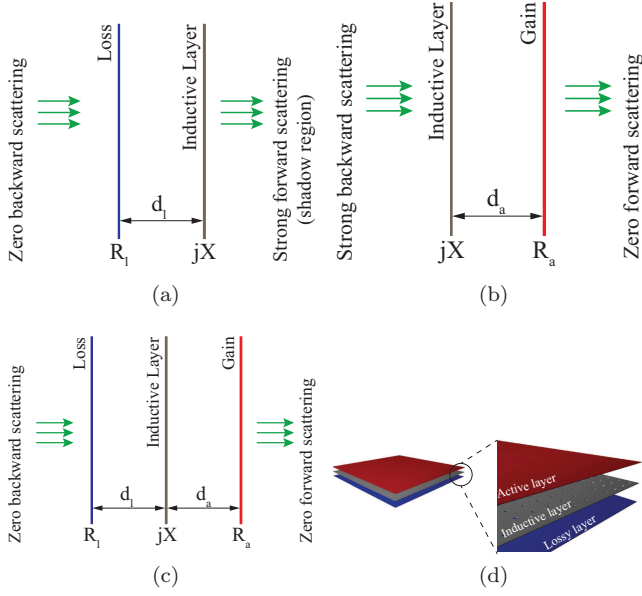


FIG. 1. Proposed geometries of interest.

ble reactance, we put a resistive sheet with the surface resistance equal to the free-space wave impedance $R_1 = \eta_0 = \sqrt{\mu_0/\epsilon_0}$ in front of the inductive layer at the distance of $d_1 = 7.5 \text{ mm} = \lambda_0/4$, as in a classical Salisbury screen [see Fig. 1(a)]. Most of the incident power is absorbed, and a negligible amount of power penetrates through the inductive film due to the very low but non-zero reactance of the inductive screen. In this design the structure suppresses backward reflection almost completely, but a nearly full shadow is still present behind the inductive sheet.

B. Engineering Transmission

In this section, we show that it is possible to engineer the shadow of a reflective mirror using a dual active structure. We go back to the original inductive layer that realizes strong reflection and shadow. Since the inductive sheet reflects nearly all the impinging power, in order to engineer the shadow, we need a secondary source behind the inductive film. As secondary source, we use an active layer with $R_a = -\eta_0$ at the same distance as in the previous example (e.i., $d_a = 7.5 \text{ mm} = \lambda_0/4$) behind the inductive screen [see Fig. 1(b)]. This layer is a time-reversed replica of the Salisbury absorber. In this active *anti-absorbing structure*, the small amount of power penetrating behind the inductive layer reaches the active layer establishing a resonating feedback loop between the inductive and active sheets. This electromagnetic whispering between the inductive and active layers continues until the anti-absorbing structure reproduces the propagating wave behind it. With the design parameters given above, the structure exhibits a resonant transmission window, creating a transmitted wave with

transmission coefficient $T = -j2$ at $f = 10 \text{ GHz}$, while from the illuminated side the structure looks like a perfect mirror [see Fig. 2]. A large amplification in transmission, which is of tunneling nature, may happen at frequencies close to the operating frequency of the structure (i.e., $f = 10 \text{ GHz}$) [see Fig. 2]. Depending on the reactance of the inductive layer, this amplification phenomenon can be tuned to any frequency close or far from the one for which the structure has been designed, and the bandwidth of the structure is entirely determined by the reactance of the inductive layer. The propagating wave behind the inductive layer may have the same or different properties than the incident wave, depending on the design parameters.

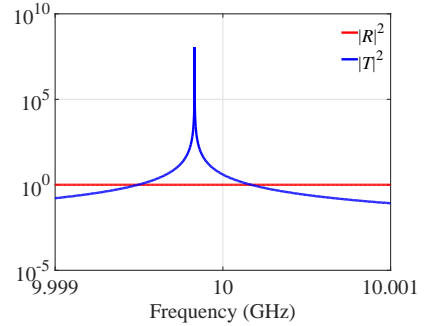


FIG. 2. Reflection and transmission coefficients for the design in Fig. 1(b).

C. \mathcal{PT} -Symmetric Teleportation

In the previous sections we considered two complementary structures: an absorbing structure to eliminate reflections from the inductive screen and an anti-absorbing structure to control the shadow behind the inductive screen. Now let us show that a structure formed by combining an absorber at the illuminated side and an anti-absorber at the shadow side eliminates both reflections and the shadow. This structure is shown in Figs. 1(c) and 1(d). We start with a design for the case of normal incidence, $R_1(\theta_i = 0^\circ) = -R_a(\theta_i = 0^\circ) = \eta_0$, and $d_1(\theta_i = 0^\circ) = d_a(\theta_i = 0^\circ) = \lambda_0/4$. The new system is now \mathcal{PT} -symmetric, since the two real impedances are opposite and the two sheets are symmetrically displaced with respect to the inductive screen. The active surface acts as the time-reversed version of the absorber. The whole structure can be viewed as a \mathcal{PT} -symmetric pair of resonators, one lossy and one active, weakly coupled through the low-reactance sheet. In the transition regime, the structure exhibits nearly zero reflection while a tiny amount of power, transmitted through the inductive screen, reaches the active layer delivering information about the incident field, and it allows synchronizing the oscillations of the active sheet with the impinging signal. Similarly to the previous case, multiple reflections

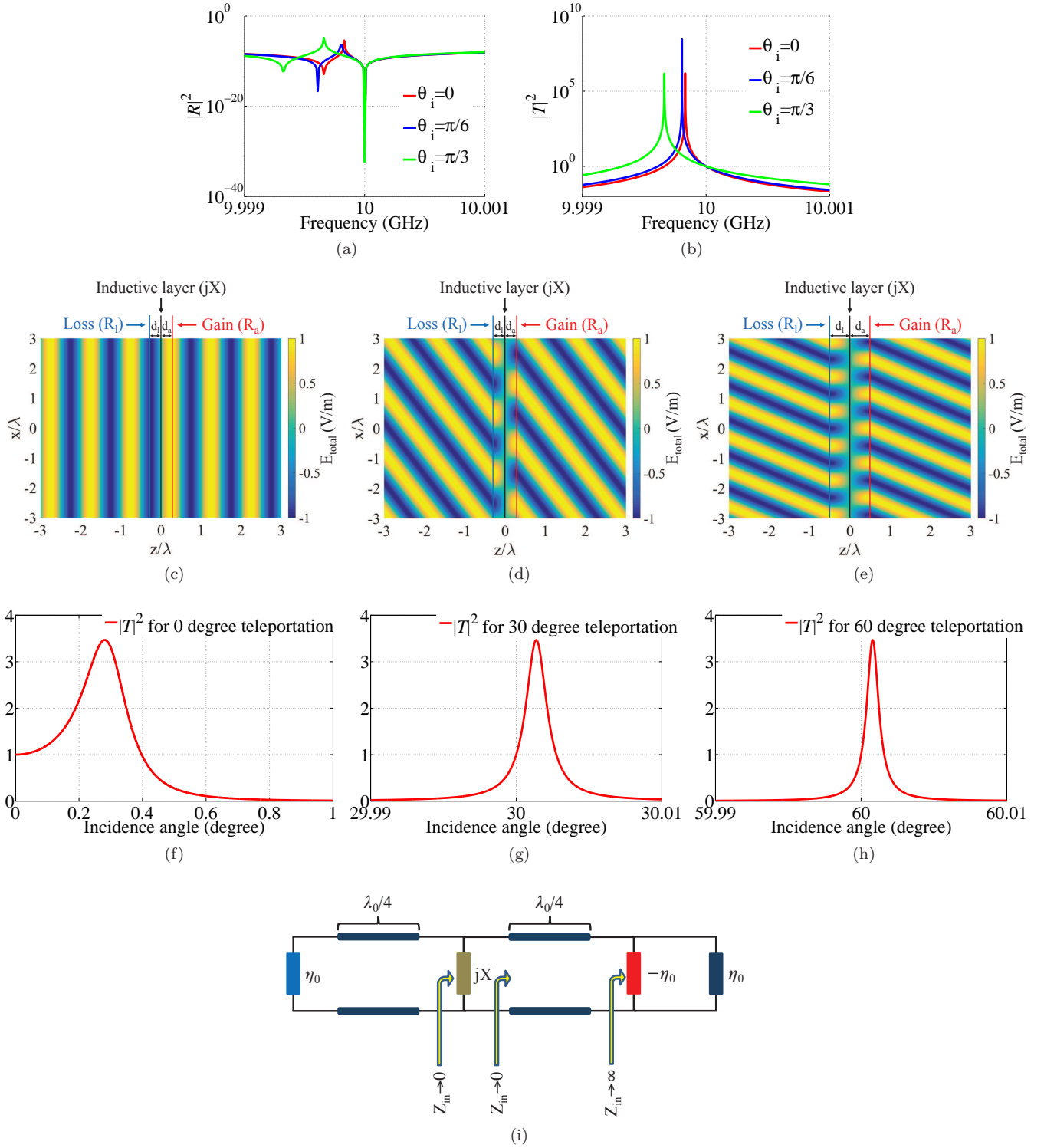


FIG. 3. (a) Reflection and (b) transmission coefficients for 0° -, 30° -, and 60° -teleportation structures (A θ_i -teleportation structure is a structure which is designed to teleport incident wave with incidence angle θ_i). Electric field distribution for (c) 0° -, (d) 30° -, and (e) 60° -teleportation structures at frequency $f = 10$ GHz. Angular dependencies for (f) 0° -, (g) 30° -, and (h) 60° -teleportation structures at frequency $f = 10$ GHz (Here, we assume that the sheet resistances are angular independent). (i) Transmission-line model for 0° -teleportation structure.

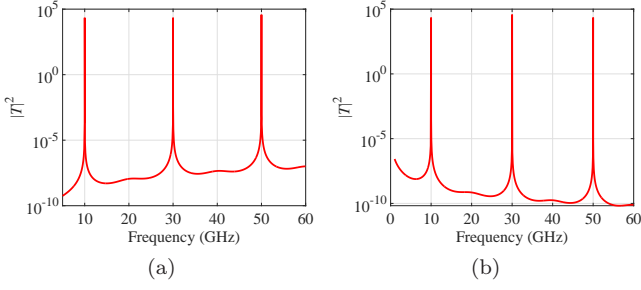


FIG. 4. Transmission coefficients for structures with (a) highly reflective inductive sheet and (b) highly reflective capacitive sheet. In both these examples $X = 0.01$ Ohm at $f = 10$ GHz.

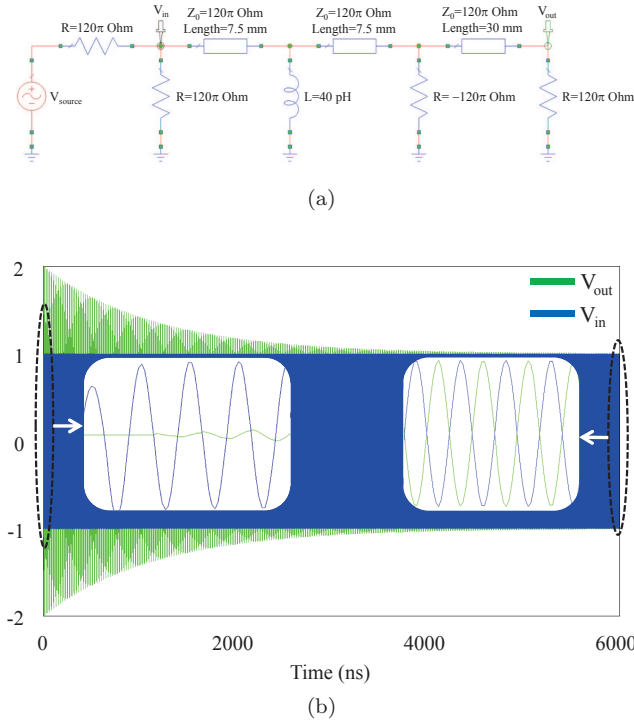


FIG. 5. Circuit model for the 0° -teleportation structure (here Z_0 is the intrinsic impedance of the transmission line and L shows the inductance of a sample inductive sheet). (b) Time-domain simulation of the circuit model (0° -teleportation structure).

inside the structure form a feedback loop channel between these two sheets. The reflection and transmission coefficients for normal incidence read

$$R = \frac{-\frac{\eta_0}{2} [1 + \cos(\pi \frac{f}{f_0})] + X \sin(\pi \frac{f}{f_0})}{\frac{\eta_0}{2} + (\frac{\eta_0}{2} + j2X) \cos(\pi \frac{f}{f_0}) + (j\eta_0 - X) \sin(\pi \frac{f}{f_0})},$$

$$T = \frac{j2X}{\frac{\eta_0}{2} + (\frac{\eta_0}{2} + j2X) \cos(\pi \frac{f}{f_0}) + (j\eta_0 - X) \sin(\pi \frac{f}{f_0})}, \quad (1)$$

where f_0 , f , and X are the frequency for which the structure has been designed, the frequency of the incident wave, and the reactance of the inductive layer, respectively. In order to get the reflection and transmission coefficients for oblique incidence, we can simply substitute f by $f \cos \theta_i$ and η_0 by $\eta_0 \cos \theta_i$ (for TM polarization) or $\eta_0 / \cos \theta_i$ (for TE polarization). The structure remains reflectionless in a fairly wide frequency range while replicating the incident wave behind the structure at a quite narrow frequency range with same amplitude and frequency [see Figs. 3(a) and 3(b)]. It should be noted that at the teleportation frequency of the structure (i.e., $f = 10$ GHz) the incident and transmitted waves are out of phase (180° phase difference), exactly the phase difference that the original plane wave would accumulate after travelling the distance between the passive and active layers. Therefore, the active structure works as a cloak, restoring the field distribution expected when the absorbing structure is removed. In some sense, this functionality resembles in one-dimensional \mathcal{PT} -symmetric cloak presented in [13] for different purposes. It is interesting to note that full power transmission happens also at another frequency, close to the resonance [Fig. 3(b)]. At that frequency, however, the power propagation channel is not closed and there is some small power transfer through the opaque sheet. The phase of the transmitted wave at this frequency approximately equals to the phase of the incident wave.

As it can be seen from Fig. 3(b), a huge amplification in transmission happens at frequencies close to the teleportation frequency. Similar to the case of the anti-absorbing structure, this amplification phenomenon is of tunneling nature and may happen at different frequencies depending on the reactance of the inductive layer. Indeed, it is interesting to investigate the physics behind this large amplification and study whether the transmission has a pole at the amplification frequency, or it is just an extremum of transmission. To this end, we can find the frequencies for which the denominator of the transmission in (1) becomes zero, i.e., when both its real and imaginary parts become zero:

$$2X \cos\left(\pi \frac{f}{f_0}\right) + \eta_0 \sin\left(\pi \frac{f}{f_0}\right) = 0, \quad (2)$$

$$\frac{\eta_0}{2} + \frac{\eta_0}{2} \cos\left(\pi \frac{f}{f_0}\right) - X \sin\left(\pi \frac{f}{f_0}\right) = 0.$$

This system of equations does not have any real solution unless when $X = 0$ for which the transmission coefficient is $T = 0$ at non-resonance frequencies. At the resonance frequency, the limiting value of T depends on the order in which we tend $f \rightarrow f_0$ and $X \rightarrow 0$ in (2). However, it is particularly interesting to explore (2) in the regime for which $X \rightarrow 0$, i.e., very small, but not zero. In this case we have an approximate solution for which the absolute value of denominator reaches its minimum (though not

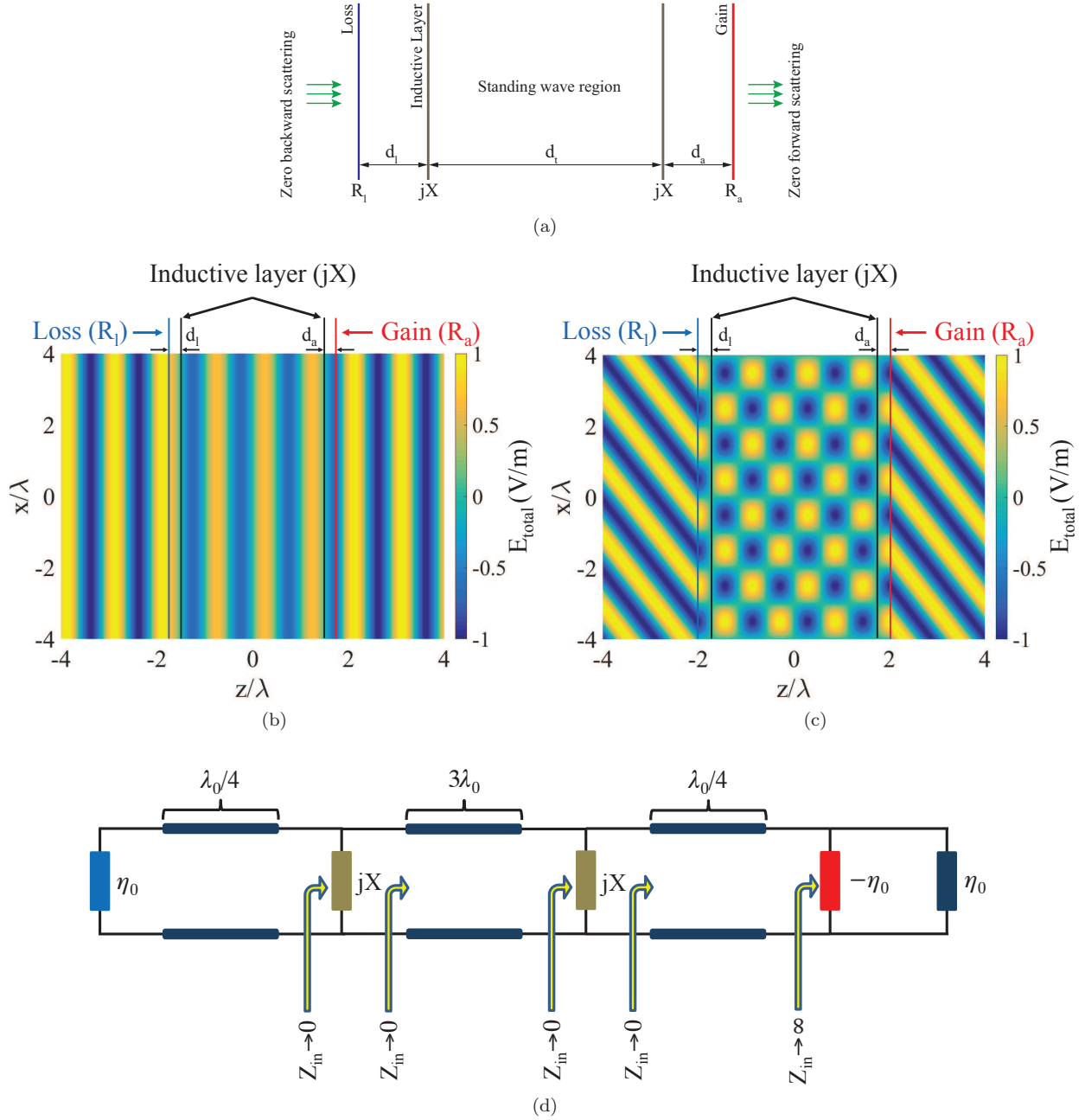


FIG. 6. (a) Geometry of the proposed long-distance-teleportation structure. Electric field distribution: (b) 0° -long-distance teleportation structure with the design parameters: $R_l = -R_a = \eta_0$, $d_l = d_a = \lambda_0/4$, $d_t = 3\lambda_0$, and $f = 10$ GHz (c) 30° -long-distance teleportation structure with the design parameters: $R_l = -R_a = \sqrt{3}\eta_0/2$, $d_l = d_a = \lambda_0/2\sqrt{3}$, $d_t = 2\sqrt{3}\lambda_0$, and $f = 10$ GHz. (d) Transmission-line model for 0° -long-distance teleportation structure.

exactly zero),

$$\pi \frac{f}{f_0} = (2m + 1)\pi - \frac{2X}{\eta_0}. \quad (3)$$

Here m is an integer. For the inductive case where $X = 2\pi fL$ (L is the surface inductance of the inductive sheet) the frequencies for which the extrema of transmis-

sion happen read

$$f = \frac{2m + 1}{1 + \frac{4L}{\eta_0}} f_0 \quad (4)$$

and for the capacitive case where $X = -1/(2\pi fC)$ (C is the surface capacitance of the capacitive sheet) the

frequencies of transmission extrema read

$$f = \left[1 + \sqrt{1 + \frac{4}{\pi^2 \eta_0 C (2m+1)^2 f_0}} \right] \frac{2m+1}{2} f_0 \quad (5)$$

It is interesting to notice that for the inductive and capacitive cases, the frequencies of transmission extrema are slightly lower and higher than the frequency of teleportation, respectively. As it can be seen from (4) and (5), the extremum of transmission is periodic with period $2f_0$ [see Fig. 4].

When X gets larger, the minimum value of the denominator deviates from zero more and more and there is no more large amplification in transmission. Within the simulated examples, the approximate results in (4) and (5) work very well, however, for large values of X these approximations are not valid any longer.

The wideband reflectionless and narrowband teleportation response of this structure can be explained in terms of the loaded quality factors of the two coupled resonators. While the lossy resonator (the resistive sheet on top of the inductive screen) has a low loaded quality factor, because the structure is well coupled to radiation modes and dissipation is high, the active resonator is weakly coupled to outside radiation and the dissipation is replaced by gain. For these reasons, the loaded quality factor of the active resonator is very high. The system acts as a series cascade of these two resonant cavities, explaining the overall narrow bandwidth of this phenomenon. The symmetry of the system is reflected in the fact that, if we excite it from the active side, we expect to see a very narrowband full transmission exactly at the same resonance of the coupled mode. The electric field distributions in Fig. 3(c) show how a normally incident wave teleports through the \mathcal{PT} -based structure.

The incident wave teleports not only over a narrow frequency range, but also in an angularly selective manner [see Fig. 3(f)]. Similar to the frequency response of the structure, a huge amplification in transmission may happen when we deviate the angle of incidence from the designed value [see Fig. 3(f)]. It should be noted that this spectrally and angularly selective structure is fundamentally different from a conventional filter, for which a change in the incidence angle would typically imply transmission at some other frequency. This unusual frequency-angle selectivity is due to the symmetry of lossy and active impedances which need to be precisely equal and opposite to the wave impedance in order to realize teleportation.

It is quite interesting to investigate what reason causes this teleportation phenomenon and what is the physics behind. Figure 3(i) shows the circuit model for this \mathcal{PT} -symmetric structure. It is seen that at the teleportation frequency of the structure (i.e. $f = 10$ GHz) the inductive impedance is shorted out. This phenomenon implies two very important points. First, the scattering parameters of the structure at the teleportation frequency are independent of the reactance of the inductive

screen, meaning that the screen can be chosen as highly conductive as we wish (of course, the reactance should not be exactly zero). This fact can be seen from (1), as well. Second, at the teleportation frequency of the structure, the passive and active sides are completely isolated and there is no connection between these two parts of the structure. It is relevant to ask how the active part of the structure can replicate the incident wave behind the structure while these two parts are electromagnetically disconnected. Do we have a tunneling mechanism or a teleportation mechanism? In other words, do we tunnel the incident wave through the structure or do we fully absorb it at the input and recreate it with the same properties at the output of the structure? To answer this question we can look at the time domain simulation of the structure. Figures 5(a) and 5(b) show the transmission-line model for the 0° -teleportation structure and the results of its time-domain simulation, respectively. It is seen that we basically have both tunneling and teleportation regimes in the structure. When we start illuminating the structure, during the transient time period (before getting to the steady state) there is a weak tunneling (plane wave propagation) between the passive and active sides which is responsible for delivering the information of the incident wave to the active side. However, as soon as the structure approaches steady state, there is no tunneling between these two parts [see the circuit model in Fig. 3(i)], the elements are fully decoupled and the structure reaches a teleportation regime in which the energy of the transmitted wave is fully fed by the active surface. In this regime, there is no power flow through the opaque screen, but it is seen that the structure is still able to completely restore the amplitude of the incident field in the shadow region. As it can be seen from the insets in Fig. 5(b), after reaching steady-state, the incident and output signals are equal in amplitude, frequency, and out of phase. Thus, the structure fully cloaks the inductive layer.

It is important to note that the structure can be designed to filter incident waves with any desired angle of incidence. For a TM incident plane wave with incidence angle θ_i to be teleported behind a low-reactance inductive layer, we just need to use lossy and active sheets with $R_i(\theta_i) = -R_a(\theta_i) = \eta_0 \cos \theta_i$ at the distances $d_i(\theta_i) = d_a(\theta_i) = \lambda_0 / (4 \cos \theta_i)$, ensuring the Salisbury condition on the passive side, and the time-reversed condition on the active side. Let us consider designs for 30° and 60° teleportation. Figures 3(a) and 3(b) show that these designs, similarly to the case of teleportation at normal incidence, exhibit a fairly broadband reflectionless regime while replicating the incident waves behind the structures in extremely narrowband frequency ranges. Electric field distributions in Figs. 3(d) and 3(e) show how the incident fields with different incidence angles are replicated at the output of the structures. Figures 3(f), 3(g), and 3(h) show that the designs for teleportation of incident waves with any angle of incidence will be angularly selective. Although up to now we have considered

only transverse-magnetic (TM) polarization for incident plane waves, by using the same methodology, this structure can be easily designed to teleport transverse-electric (TE) incident plane waves with arbitrary incidence angles.

When the system, designed to teleport waves at a specific frequency and at a specific incidence angle, is illuminated from the opposite side (the side of the active sheet), the same phenomenon of frequency- and angular-selective complete teleportation is observed at the same frequency and for the same incidence angle, as expected from reciprocity. However, in this case the reflection is not minimized, but, in contrast, the system strongly amplifies the reflected power.

D. Long-Distance \mathcal{PT} -Symmetric Teleportation

At this point, an interesting question arises of whether it is possible to locate lossy and active parts of the structure far away from each other, and still teleport the incident wave. Figure 6(a) shows a \mathcal{PT} -symmetric structure in which the lossy and active parts are located at the distance $3\lambda_0$. Electric field distribution in Fig. 6(b) shows that incident electromagnetic waves can fully teleport through the structure. Again, also this long-distance teleportation system can be designed to teleport electromagnetic plane waves at any desired angle of incidence [e.g., see Fig. 6(c) for 30° teleportation]. As it can be seen from the transmission-line model of the structure in Fig. 6(d), in the steady-state regime, the inductive loads are shorted out, meaning that there is no power flow from the passive side toward the active one. Instead, there is a standing wave between the two inductive layers [see Figs. 6(b) and 6(c)]. It should be noted that teleportation structures can be designed to teleport incident electromagnetic waves over longer distances $d_t = n\lambda_0/(2 \cos \theta_i)$ where n is an integer. This way we can absorb electromagnetic waves at one surface and recreate it at a distance far away from the surface. Moreover, in this scenario we are able to excite oscillations inside the resonator (the cavity between the two conductive sheets) which has an infinitely high quality factor at the resonance frequency. Indeed, as discussed above, in the steady-state regime, even the tiny holes in both sheets are effectively closed (shorted out), due to the presence of the active sheet at the quarter-wave distance. Similarly to the teleportation through a single sheet, the energy is pumped into the resonator during the transient period, while in the steady-state regime the cavity is completely isolated from the environment.

The unique properties of the proposed \mathcal{PT} -symmetric layer suggest interesting application possibilities, e.g., in selective sensors. Note that, in contrast to known angular-selective filters (for example, based on photonic crystals [15]), which reflect waves coming from directions other than the one for which they are designed, the proposed \mathcal{PT} -symmetric filter absorbs them. Non-reflecting fil-

ters are advantageous in privacy-protecting devices and in sensor applications. Frequency- and angular-selective resonant amplification phenomenon suggests novel opportunities in boosting sensor sensitivity and in the creation of various nonlinear devices [16].

The active sheets in the proposed \mathcal{PT} -symmetric teleportation structures can be realized using an array of dipoles loaded with negative resistors. At RF and low microwave frequencies, negative resistance devices can be realized using impedance inverter circuits (amplifiers with appropriate feedback networks). At higher microwave frequencies one can use semiconductor components, e.g. tunnel or Gunn diodes [17]. In the infrared or visible range, various optically pumped gain media can be used.

Here we have based our discussion on a pair of Salisbury-type absorber and a corresponding anti-absorber. However, the same concept can be applied to a pair of Dallenbach absorber [18] and anti-absorber or any other type of absorbers [19] paired with their time-reversed image to form a \mathcal{PT} -symmetric pair. For example, instead of the topology shown in Fig. 1(c), one can position a lossy dielectric slab of the quarter-wave thickness with the refractive index $n_{\text{Lossy}} \approx \pi/(2k_0d) - j2/\pi$ (e.g., see Sec. 12.3 in [20]) in front and an active slab with refractive index of $n_{\text{Active}} \approx \pi/(2k_0d) + j2/\pi$ and the same thickness behind the inductive layer and still teleport the incident wave behind the inductive layer. In this scenario, the same amount of power absorbed at the lossy side of the structure is reproduced at the active side of the structure. The active layer in this structure can, for example, be realized using an optically pumped semiconductor layer structure.

III. CONCLUSIONS

In conclusion, we have described the phenomenon of full teleportation of electromagnetic waves based on \mathcal{PT} -symmetric one-dimensional geometries, able to eliminate both backward and forward scattering from a nearly fully reflective layer. It was shown that the electromagnetic whispering between the lossy and active sheets in the transient regime is enough to deliver the information on the amplitude and phase of the incident wave to the active side of the \mathcal{PT} -symmetric teleporting structure. However, in the steady-state regime the passive and active parts of the \mathcal{PT} -symmetric teleporting structures are electromagnetically disconnected and the active part of the structure completely recreates the incident wave behind the structure based on the information which had been delivered during the transient regime time. This feature makes the proposed structure quite different from tunneling structures where the incident field tunnels through and reaches the output of the structure. We have generalized this concept to teleport electromagnetic waves over long distances, in which electromagnetic waves can be absorbed at one side and

be reproduced at the other side, which can be far away from the entry point. **Although in this paper we utilized**

a pair of Salisbury-type absorber and a corresponding anti-absorber, the proposed concept can be applied to any pair of absorber and anti-absorber.

-
- [1] L. Zhou, W. Wen, C. T. Chan, and P. Sheng, “Electromagnetic-wave tunneling through negative-permittivity media with high magnetic fields,” *Phys. Rev. Lett.*, vol. 94, no. 24, p. 243905, 2005.
- [2] D. L. Gao, L. Gao, and C. W. Qiu, “Birefringence-induced polarization-independent and nearly all-angle transparency through a metallic film,” *EPL*, vol. 95, no. 3, p. 34004, 2011.
- [3] A. Alù and N. Engheta, “Pairing an epsilon-negative slab with a mu-negative slab: Resonance, tunneling and transparency,” *IEEE Trans. Antennas Propag.*, vol. 51, no. 10, pp. 2558–2571, 2003.
- [4] G. Castaldi, V. Galdi, A. Alù, and N. Engheta, “Electromagnetic tunneling of obliquely incident waves through a single-negative slab paired with a double-positive uniaxial slab,” *J. Opt. Soc. Am. B*, vol. 28, no. 10, pp. 2362–2368, 2011.
- [5] S. Savoia, G. Castaldi, V. Galdi, A. Alù, and N. Engheta, “Tunneling of obliquely incident waves through \mathcal{PT} -symmetric epsilon-near-zero bilayers,” *Phys. Rev. B*, vol. 89, p. 085105, 2014.
- [6] T. Feng, Y. Li, H. Jiang, Y. Sun, L. He, H. Li, Y. Zhang, Y. Shi, and H. Chen, “Electromagnetic tunneling in a sandwich structure containing single negative media,” *Phys. Rev. E*, vol. 79, no. 2, p. 026601, 2009.
- [7] L. Feng, Z. J. Wong, R. -M. Ma, Y. Wang, and X. Zhang, “Single-mode laser by parity-time symmetry breaking,” *Science*, vol. 346, pp. 972–975, 2014.
- [8] B. Peng, Ş. K. Özdemir, F. Lei, F. Monifi, M. Gianfreda, G. L. Long, S. Fan, F. Nori, C. M. Bender, and L. Yang, “Parity-time-symmetric whispering-gallery microcavities,” *Nature Physics*, vol. 10, pp. 394–398, 2014.
- [9] Z. Lin, H. Ramezani, T. Eichelkraut, T. Kottos, H. Cao, and D. N. Christodoulides, “Unidirectional invisibility induced by \mathcal{PT} -symmetric periodic structures,” *Phys. Rev. Lett.*, vol. 106, p. 213901, 2011.
- [10] R. Fleury, D. L. Sounas, and A. Alù, “Negative refraction and planar focusing based on parity-time symmetric metasurfaces,” *Phys. Rev. Lett.*, vol. 113, p. 023903, 2014.
- [11] A. Regensburger, C. Bersch, M. -A. Miri, G. Onishchukov, D. N. Christodoulides, and U. Peschel, “Parity-time synthetic photonic lattices,” *Nature*, vol. 488, pp. 167–171, 2012.
- [12] L. Feng, Y. -L. Xu, W. S. Fegadolli, M. -H. Lu, J. E. B. Oliveira, V. R. Almeida, Y. -F. Chen, and A. Scherer, “Experimental demonstration of a unidirectional reflectionless parity-time metamaterial at optical frequencies,” *Nature Materials*, vol. 12, pp. 108–113, 2013.
- [13] D. L. Sounas, R. Fleury, and A. Alù, “Unidirectional cloaking based on metasurfaces with balanced loss and gain,” *Phys. Rev. Appl.*, vol. 4, no. 1, p. 014005, 2015.
- [14] W. W. Salisbury, Absorbent body of electromagnetic waves, U.S. Patent 2 599 944 (10 June 1952).
- [15] Y. Shen, D. Ye, I. Celanovic, S. G. Johnson, J. D. Joannopoulos, and M. Soljačić, “Optical broadband angular selectivity,” *Science*, vol. 343, pp. 1499–1501, 2014.
- [16] R. Fleury, D. Sounas, and A. Alù, “An invisible acoustic sensor based on parity-time symmetry,” *Nature Communications*, vol. 6, p. 5905, 2015.
- [17] **T. Jiang, K. Chang, L. -M. Si, L. Ran, and H. Xin, “Active microwave negative-index metamaterial transmission line with gain,” *Phys. Rev. Lett.*, vol. 107, no. 20, p. 205503, 2011.**
- [18] **W. Dallenbach and W. Kleinsteuber, “Reflection and absorption of decimeter-waves by plane dielectric layers,” *Hochfreq. u. Elektroak.*, vol. 51, pp. 152–156, 1938.**
- [19] **Y. Ra’di, C. R. Simovski, and S. A. Tretyakov, “Thin perfect absorbers for electromagnetic waves: Theory, design, and realizations,” *Phys. Rev. Applied*, vol. 3, p. 037001, 2015.**
- [20] **A. N. Serdyukov, I. V. Semchenko, S. A. Tretyakov, and A. Sihvola, *Electromagnetics of Bi-Anisotropic Materials: Theory and Applications.*, Amsterdam, The Netherlands: Gordon and Breach, 2001.**